Al-Khwarizmi Engineering Journal
ISSN (printed): 1818 – 1171, ISSN (online): 2312–0789
Vol. 21, No. 1, March (2025), pp. 61– 72

Al-Khwarizmi Engineering Journal

# Improving the Performance of Steering by Wire Using a Model Predictive Controller Enhanced with Particle Swarm Optimisation

**Taher Sachit Taher[1], Ali Hussien Mary[2*], Furat Ibrahim Hussein[3], Mohammed Ghufran Khidhir Abboosh[4] and Muhammad Umar Fareed[5]**

*[1,2,3] Department of Mechatronics Engineering, Al-Khwarizmi College of Engineering, University of Baghdad, Baghdad, Iraq*
*[4] Department of Data Science and Visualization, University of Debrecen, Hungary*
*[5] Wakefield College, Wakefield, England*
*Corresponding Author's Email: alimary76@kecbu.uobaghdad.edu.iq

(Received 7 August 2024; Revised 28 December 2024; Accepted 27 January 2025; Published 1 March 2025)
**https://doi.org/10.22153/kej.2025.01.002**

## Abstract

The challenges of steering-by-wire (SBW) systems in vehicles are due to the absence of a direct mechanical link between the steering wheel and the wheels on the road. This limitation imposes the necessity of employing sophisticated control systems to attain the highest accuracy and stability during operation. In such systems, the responsibility rests completely on the utilised controller to change the wheel's angle on the road swiftly and accurately in response to the steering wheel changes by the driver. However, conventional control systems suffer slowly in responding to instructions and some fixed errors in their steady-state phase. The current study introduces an innovation of a model that integrates model predictive control (MPC) with particle swarm optimisation (PSO) to improve the performance of SBW systems. The MPC procedure is typically employed to control system responses over a timeframe and eliminate unnecessary and ineffective actions according to the specified objectives. The PSO algorithm is used to manage the ineffective parameters within the MPC. Results revealed that the proposed approach remarkably and effectively shortens response time, enhances wagon stability and reduces the settling error to nearly null. In addition, the integration of PSO with the overall system performance enhances the tuning of the response time, hence augmenting the system efficiency and responsiveness. The study outcomes support the proposal that the control strategy can improve the efficiency of SBW systems with high operational goals.

***Keywords:*** *Steering by wire; Vehicle; Model predictive controller; Particle swarm optimisation; Controller.*

## 1. Introduction

Steering-by-wire (SBW) systems are a promising steering system technology in the field of automotive and transportation industry. Such systems found their way largely into automatic guided vehicle (AGV) systems, fork lifters and many material handling instrument control strategies that have been implemented over the years to improve their performance. SBW does away with the direct mechanical hardware between the steering wheel and the wheels on the road. This innovation must be precise enough and has an extremely fast response speed to ensure high-resolution operational performance, which will satisfy drivers and users whilst ensuring safety [1].

Early SBW systems used classic proportional integral derivative (PID) controllers, which provide acceptable performance for numerous linear systems. When they are integrated with nonlinearities and time delays or applied in changing operating conditions, they lose their efficiency. Åström et al. and Mary et al. [2–3] stated that PID controllers usually do not work well in dynamic environments due to their issues with stability and accuracy, which affect error rate growth.

Fuzzy logic controllers are more suitable for complex and nonlinear systems because of their ability to tolerate instability and loss choices. Mitra and Kumar [4] improved the flexibility and robustness of fuzzy logic controllers in SBW systems, especially under the conditions of long disturbances and disturbing impacts. Despite these exceptional features, the layout of lean logic controllers can be troublesome, and fine-tuning them is necessary to ensure proper use [5].

Flexible control strategies are created as a response to the shortcomings of traditional control procedures. Adaptive control frameworks robustly change their parameters to adapt to modifications in dynamic systems [6]. The use of adaptive control in many applications has improved accuracy and robustness against disturbances [7–8]. Similarly, Gao et al. [9] studied the integration of adaptive control into robotic systems, which resulted in enhanced efficiency and reduced error rates. Using console-based artificial intelligence, such as neural networks, deep learning and reinforcement learning, can enhance responsiveness to data and improve performance over time; however, it requires substantial computing power and massive training data [10].

The most prominent advanced control technology used to improve the performance of transmission lines is model predictive control (MPC). It represents a control strategy that can deal with a wide range of constraints and achieve the optimal performance in dynamic environments. MPC operates by predicting the enduring temporal behaviour of the framework based on a scientific model and thereafter determining the most suitable control strategies to achieve the desired performance. Control activities occur intermittently, enabling the system to repair deviations and maintain the target state efficiently. MPC has been utilised in various contexts, including its implementation in thermal management systems for business process optimisation, thereby enhancing system stability and reducing energy consumption in automotive systems [7]. It works by anticipating the long-standing time behaviour of the framework based on a scientific demonstration and then calculating the foremost fitting control methods to realise the focus on execution. Control activities happen intermittently, permitting the framework to rectify deviations and keep up the target state productively. MPC has been used in several settings, proven using MPC in thermal management structures in business procedure manipulate [11], which stepped forward system stability and decreased electricity consumption in car systems [12] showed that MPC can provide an automotive manipulate gadget advanced in the field of robotics [13]. For direction planning and impediment avoidance based totally on MPC, leading to green and safe robots[14].

Ates et al. [15] tested the usage of MPC in thermal control structures, which showed high adaptability to surprising environmental adjustments, improving gadget stability and reducing energy intake. Similarly, Ye et al. [16] showed that MPC can enhance the performance of visitor control systems, thereby improving high-quality-grained making plans and rapid reaction to adjustments in overall performance.

Particle swarm optimisation (PSO) is a popular algorithm specifically designed for the social behaviour of birds and fish. It enhances problem solving by allowing proposed solutions, known as particles, to move in the search space in line with simple mathematical principles based on their most useful function and the optimal function of the system. Therefore, this collective behaviour contributes to finding the most useful solution efficiently. It has demonstrated efficacy in addition to systems that improve management systems in many packages. PSO has been used to optimise the control parameters of automated drive structures [17], resulting in improved accuracy and responsiveness. In power structures, PSO is used to enhance load distribution hassles, obtaining improved performance and electrical efficiency [18], [15], [19].

Kumar and Sharma [20] tried optimising the MPC parameters using PSO, thereby improving overall implementation at scale and reaching faster response states and better tuning in active situations. Based on these effects, this consideration suggests combining MPC and PSO to increase the dominant control framework. A mathematical model of the device can be developed [21], and its performance can be analysed using MPC, with PSO used to optimise control parameters. The abovementioned integrated approach is expected to enhance the device's high accuracy and responsiveness, giving it extraordinarily high effectiveness in commercial and transportation software. The integration of MPC and PSO provides a synergistic effect, combining the predictive and constraint processing skills of MPC with the optimisation ability of PSO. This technique has a high ability to overcome many challenging situations in the SBW system, including dealing with nonlinearities, uncertainties and external disturbances. By leveraging the strengths of both technologies, the proposed controller aims to have superior overall performance and reliability. The effectiveness of mixing MPC and PSO has been explored in many research. Huang et al. [22] conducted a comparative assessment of assembled optimisation calculations comprising PSO in tuning MPC parameters for chemical system organisation, thus determining crucial developments in execution estimations. In the setting of SBW systems, Yan et. al. [23] reviewed the application of MPC for road checking in AGVs, fulfilling tall exactness and quality to unsettling impacts. Complementarily, Tavoosi et al. [24] utilised PSO to make strides in the course arrangement of AGVs, resulting in smoother and more proficient directions.

The present study aims to develop and evaluate a mathematical model concentrating on applying MPC-PSO in SBW systems. The objective is to expect and control system conduct, using PSO to optimise MPC management parameters and comparing the performance of the included machine through simulations and experimental verification. A complex control system that remarkably fulfils the accuracy and responsiveness demands of advanced commercial and transportation solutions is expected.

## 2. Modelling of SBW Systems

The hardware of SBW systems has three fundamental subsystems, each containing many sensors or actuators, as shown in Figure 1. The assembly of the steering wheel, the front wheel subsystem and some additional mechanical hardware. The guidance wheel includes a torque sensor, a steering attitude sensor and maybe a movement encoder. The front wheel system accommodates an angle sensor, a motor encoder, rack equipment and additives of the wheel suspension system.

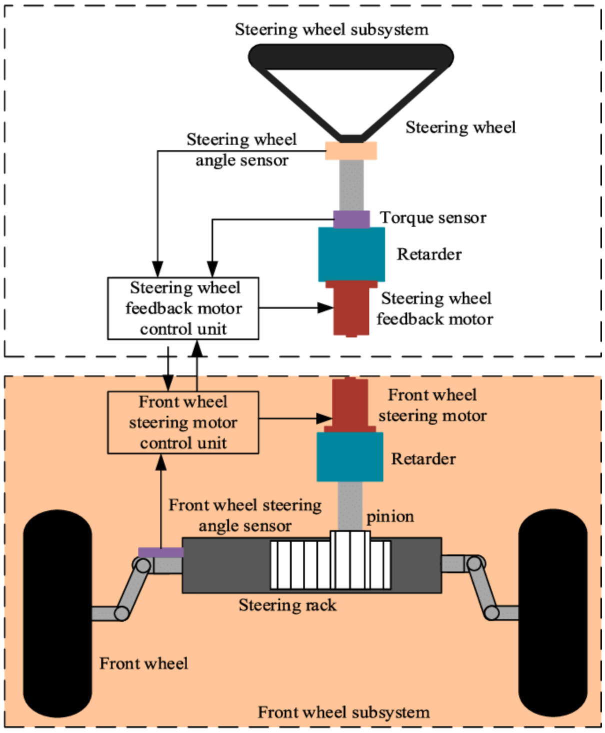


**Fig. 1. Steering-by-wire System [2]**

### 2.1 Modelling of the Steering Wheel

A schematic of the steering wheel assembly in Figure 2 indicates that the system is associated with many considered variables, i.e., steering angle, steering motor angle and current, with other inputs including motor voltage, input angle, torque and friction torque produced during wheel rotation. The system's dynamic model can be expressed in accordance with Newton's laws, as shown in the series of equations below.

The angle of the steering wheel, the angular displacement of the steering motor and the steering motor current can be stated as [21]

$$\ddot{\theta}_s = 1/J_s(T_{driver} - T_{friction} - b_{sc} * \dot{\theta}_s - k_s * \theta_s + b_{sc} * \dot{\theta}_{m1} + k_s * \theta_{m1}), \quad \ldots (1)$$

$$\ddot{\theta}_s = 1/J_s(T_{driver} - T_{friction} - b_{sc} * \dot{\theta}_s - k_s * \theta_s + b_{sc} * \dot{\theta}_{m1} + k_s * \theta_{m1}), \quad \ldots(2)$$

$$\frac{di_1}{dt} = 1/L_1(-R_1 * i_1 - K_{b1} * \dot{\theta}_{m1} + V_{s1}), \quad \ldots(3)$$

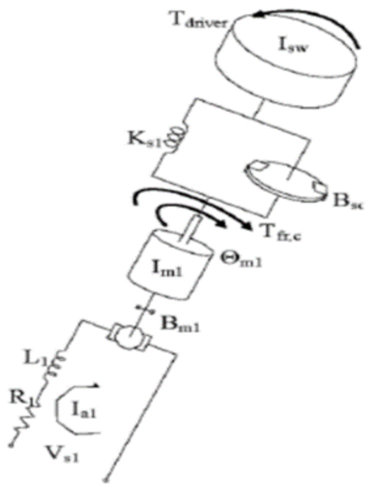


**Fig. 2. Steering Wheel Subsystem Diagram [25]**

Torque of Steering Motor [26]

$$T_{m1} = K_t * i_1. \qquad \dots (4)$$

Accordingly, the state space representation of the steering wheel system can be expressed as follows:

$$\ddot{X}(t) = A_s X(t) + B_s U(t), \qquad \dots (5)$$

Output

$$y(t) = C_s X(t) + D_s\, U(t), \qquad \dots (6)$$

State

$$X(t) = \left[\Theta_s\ \dot{\Theta}_s\ \Theta_{m1}\ \dot{\Theta}_{m1}\ i_1\ \right]^T. \qquad \dots (7)$$

The inputs include the driver torque ($T_{driver}$), friction torque ($T_{friction}$) and motor voltage ($V_{s1}$):

$$U(t) = [T_{driver}\ T_{friction}\ V_{s1}\ ]^T, \qquad \dots (8)$$

$$A_s = \begin{bmatrix} 1 & 0 & 0 & 0 & 0 \\ \left(-\frac{Ks}{Js}\right) & \left(-\frac{bsc}{Js}\right) & \left(\frac{Ks}{Js}\right) & \left(\frac{bsc}{Js}\right) & 0 \\ 0 & 0 & 0 & 1 & 0 \\ \left(\frac{Ks}{Jm1}\right) & \left(-\frac{bsc}{Jm1}\right) & \left(-\frac{Ks}{Jm1}\right) & \left(-\frac{(bm1+bsc)}{Jm1}\right) & 0 \\ 0 & 0 & 0 & \left(\frac{-Kb1}{L1}\right) & \left(\frac{-R1}{L1}\right) \end{bmatrix}, \qquad \dots (9)$$

$$B_s = \begin{bmatrix} 0 & 0 \\ \left(\frac{(Tdriver-Tfriction)}{Js}\right) & 0 \\ 0 & 0 \\ 0 & 0 \\ 0 & \left(\frac{1}{L1}\right) \end{bmatrix} \qquad \dots (10)$$

The angle and current of the steering motor are the outputs of the system.

$$C_s = \begin{bmatrix} 0 & 0 & 1 & 0 & 0 \\ 0 & 0 & 0 & 0 & 1 \end{bmatrix} \qquad \dots (11)$$

$$D_s = 0$$

where $\Theta_s$ (degree) is the angular displacement of the steering wheel, $\Theta_{m1}$ (degree) is the angular displacement of the front wheel motor, $i_1$ (A) is current of steering motor, Ks (N.m/Rad) is lumped torque stiffness, bsc (N.ms/Rad) is steering column damping, bm1 (N.m.s/Rad) is motor damping, Js (Kg.m$^2$) is steering lumped inertia, Jm1 (Kg.m$^2$) is steering motor inertia, Kb1 (V) is steering motor emf constant, L1 (H) is steering motor electrical inductance and R1 (Ohm) is steering motor electrical resistance.

## 2.2 Front Wheel Subsystem Modelling

As shown in Figure 3, the yaw angle ($\gamma_{rack}$), front wheel angle ($\delta_f$) and front motor angle ($\Theta_{m2}$) are the key variables in representing the front wheel subsystem. The force of the rack and the angle of the front tire can be represented by [27]:

$$\dot{\gamma}_{rack} = -\frac{br}{mr}\gamma_{rack} - \frac{\Theta_{m2}}{C_{m2}*g_m} - \frac{g_r}{c_t}v_t \qquad \dots (12)$$

$$\dot{\delta}_f = -\frac{B_t}{J_t}\delta_f + \frac{v_t}{c_t} \qquad \dots (13)$$

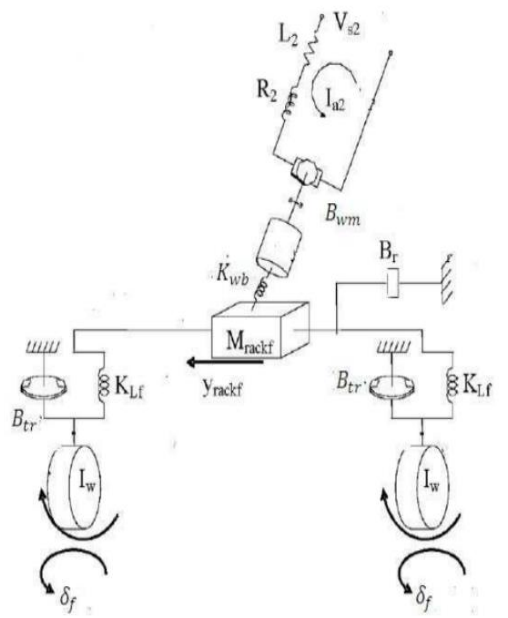


**Fig. 3. The Front Wheel Subsystem diagram [25].**

The current, torque, angular displacement of the front motor and velocity of the tire rod are stated as [27]:

$$\frac{di_2}{dt} = 1/L_2(-R_2 * i_2) - \frac{K_{b2}}{J_{m2}} * \mathrm{T}_{m2} + V_{s2} \qquad \dots (14)$$

$$\dot{T}_{m2} = \frac{k_{b2}}{L_2} * i_2 - \frac{b_{m2}}{J_{m2}} * \mathrm{T}_{m2} - \frac{\Theta_{m2}}{C_{m2}} \qquad \dots (15)$$

$$\dot{\Theta}_{m2} = \frac{T_{m2}}{J_{m2}} + \frac{\gamma_{rack}}{m_r * g_m} \qquad \dots (16)$$

$$\dot{v}_t = \frac{\gamma_{rack}}{m_r * g_r} - \frac{v_t}{j_t} \quad \dots (17)$$

The state space model of the front wheel subsystem is

$$\ddot{X}(t) = A_f X(t) + B_f U(t) \cdot \quad \dots (18)$$

The output angle of the steering motor represents the input to the front wheel subsystem:

$$U(t) = [\, \Theta_{m1} \,]^T \cdot$$

The output and state of the front wheel subsystem:

$$y(t) = C_f X(t) + D_f\, U(t) \quad \dots (19)$$

$$X(t) = [i_2 \;\; T_{m2}\; \gamma_{rack}\; \delta_f\; \Theta_{m2}\; v_t]^T \quad \dots (20)$$

The outputs of the front wheel system are the front motor angle and the wheel angle:

$$A_f = \begin{bmatrix} \left(-\frac{R2}{L2}\right) & \left(-\frac{Kb2}{Jm2}\right) & 0 & 0 & 0 & 0 \\ \left(\frac{Kb2}{L2}\right) & \left(-\frac{bm2}{Jm2}\right) & 0 & 0 & \left(-\frac{1}{Cm2}\right) & 0 \\ 0 & 0 & 0 & \left(-\frac{Bt}{Jt}\right) & 0 & \left(\frac{1}{Ct}\right) \\ 0 & \left(\frac{1}{Jm2}\right) & \left(-\frac{1}{gm+mr}\right) & 0 & 0 & 0 \\ 0 & 0 & \left(\frac{1}{gr+mr}\right) & \left(-\frac{1}{Jt}\right) & 0 & 0 \end{bmatrix}, \quad \dots (21)$$

$$B_f = \begin{bmatrix} 1 \\ 0 \\ 0 \\ 0 \\ 0 \end{bmatrix}, \quad \dots (22)$$

$$C_f = \begin{bmatrix} 0 & 0 & 0 & 1 & 0 & 0 \\ 0 & 0 & 0 & 0 & 1 & 0 \end{bmatrix}, \quad \dots (23)$$

$$D_f = 0,$$

where br (N.m/Rad) is the resistance rack, mr (Kg) is the mass rack, cm2 (N.m/s) is the front motor shaft compliance, gm (m) is the column pinion radius, gr (m) is the length ratio steering arm, ct (Rad/N.m) is the compliance of the tire rod, Bt (N.m.s/Rad) is the resistance of the tire rod, Jt (Kg.$m^2$) is the inertia of tire, vt (Km/h) is the tire rod velocity, Kb2 (V) is the front-wheel motor emf constant, Jm2 (Kg.$m^2$) is the front motor inertia, and bm2 (N.m.s/Rad) is the front motor damping.

## 3. Controller Design

This stage discusses the plan of a controller that coordinates MPC with PSO to obtain accurate and appropriate control over the routing framework. This approach leverages the prescient and controlling gifts of MPC in conjunction with the parameter optimisation qualities of PSO to pick up the most dependable execution.

### 3.1 MPC Algorithm

One effective and adaptable control method that is frequently applied to dynamic systems is MPC. It works especially well in situations such as SBW systems where managing restrictions is essential. Using a mathematical model, MPC forecasts a system's future behaviour and determines the best course of action for control to reach the intended performance.

To minimise a cost function, which usually represents the departure from the intended system trajectory whilst considering system restrictions, MPC solves an optimisation problem at each time step.

This control strategy is based on the representation of system dynamics using a state space model.

The basic model utilised in MPC, which is typically described in the state space form, must be presented before going into the specific mathematical formulation.

The system dynamics in MPC consists of system matrices A,B,and C[7][8][11][15]:

$$Z_{k+v|k} = CA^v X_k + [CA^{v-1}\;\; CA^{v-2}B \;\dots CAB\;\; CB] \begin{bmatrix} U_{k|k} \\ U_{k+1|k} \\ U_{k+2|k} \\ \cdot \\ \cdot \\ \cdot \\ U_{k+v-2|k} \\ U_{k+v-1|k} \end{bmatrix}, \quad \dots (24)\ [16]$$

where $Z_k \in \mathbb{R}^r$ is the output that needs to be controlled, and $v$ is the control horizon.

The predictive for the final step (k+f) can be obtained by

$$Z_{k+f|k} = CA^f X_k + [CA^{f-1}\;\; CA^{f-2}B \dots CA^{f-v+1}B\;\; C\bar{A}_{f,v}B] \begin{bmatrix} U_{k|k} \\ U_{k+1|k} \\ U_{k+2|k} \\ \cdot \\ \cdot \\ \cdot \\ U_{k+v-2|k} \\ U_{k+v-1|k} \end{bmatrix}, \quad \dots (25)[16]$$

$$Z = OX_k + MU\,, \quad \dots (26)[16][19]$$

$$Z = \begin{bmatrix} Z_{k+1|k} \\ Z_{k+2|k} \\ Z_{k+3|k} \\ \cdot \\ \cdot \\ Z_{k+v|k} \\ Z_{k+v+1|k} \\ \cdot \\ \cdot \\ Z_{k+f|k} \end{bmatrix}, \quad U = \begin{bmatrix} U_{k|k} \\ U_{k+1|k} \\ U_{k+2|k} \\ \cdot \\ \cdot \\ \cdot \\ U_{k+v-2|k} \\ U_{k+v-1|k} \end{bmatrix}, \quad O = \begin{bmatrix} CA \\ CA^2 \\ CA^3 \\ \cdot \\ \cdot \\ CA^v \\ CA^{v+1} \\ \cdot \\ \cdot \\ CA^f \end{bmatrix}, \quad \dots (27)[20]$$

$$M = \begin{bmatrix} CB & 0 & 0 & 0 & \dots & 0 \\ CAB & CB & 0 & 0 & \dots & 0 \\ CA^2B & CAB & CB & 0 & \dots & 0 \\ \cdot & \cdot & \cdot & & & \cdot \\ \cdot & \cdot & \cdot & \dots & \dots & \cdot \\ \cdot & \cdot & \cdot & & & \cdot \\ CA^{v-1}B & CA^{v-2}B & CA^{v-3}B & \dots & CAB & CB \\ CA^vB & CA^{v-1}B & CA^{v-2}B & \dots & CA^2B & C\bar{A}_{1,v}B \\ \cdot & \cdot & \cdot & & & \cdot \\ \cdot & \cdot & \cdot & \dots & \dots & \cdot \\ \cdot & \cdot & \cdot & & & \cdot \\ CA^fB & CA^{f-1}B & CA^{f-2}B & \dots & CA^{f-v+1}B & C\bar{A}_{f,v}B \end{bmatrix}, \quad \dots (28)[22]$$

where M is a state prediction matrix.

Let these desired outputs be denoted by

$$Z^d{}_{k+1}, Z^d{}_{k+2}, Z^d{}_{k+3}, \dots\dots\dots, Z^d{}_{k+f}, \quad \dots (29)[23]$$

$$Z^d = \begin{bmatrix} Z^d{}_{k+1} \\ Z^d{}_{k+2} \\ Z^d{}_{k+3} \\ \cdot \\ \cdot \\ \cdot \\ \cdot \\ Z^d{}_{k+f} \end{bmatrix} \cdot \quad \dots (30)[28]$$

The cost function can be expressed as [29]

$$min_U \|Z^d - Z\|_2 = min_U \left(Z^d - Z\right)^T (Z^d - Z) \cdot \quad \dots (31)$$

By substituting $Z^d$ and $Z$, the final form of the cost function that will penalise the inputs becomes clear as shown in the following equation:

$$J_U = U^T W_3 U, \quad \dots (32)$$

where $J_U$ is a cost function for control input, U is an input vector control, and $W_3$ is a final weighting matrix.

$$W_3 = W^T{}_1 W_2 W_1 \quad \dots (33)[30][7]$$

$$W_2 = \begin{bmatrix} Q_0 & 0 & 0 & .. & .. & 0 \\ 0 & Q_1 & 0 & .. & .. & 0 \\ 0 & .. & . & .. & .. & 0 \\ . & .. & .. & . & .. & . \\ . & .. & .. & .. & . & . \\ 0 & 0 & 0 & .. & .. & Q_{v-1} \end{bmatrix} \quad \dots (34)$$

Matrix dimensions are $W_2 = [m * n, m * n]$, where $W_1$, $W_2$, m and n are the state prediction matrix, input weight matrix, number of outputs and number of inputs, respectively.

The cost function that corresponds to the tracking error is

$$J_z = (S - MU)^T W_4 (S - MU), \quad \dots (35)[7]$$

Where $(S = Z^d - OX_k)\cdot$

The cost function penalises the difference between the desired and controlled trajectory as shown in the following equation [7]:

$$min_U J_z + J_U \cdot \quad \dots (36)$$

By partial derivative of the cost function for U,

$$\frac{\partial J}{\partial U} = -2M^T W_4 + 2M^T W_4 M U + 2W_3 U \cdot \quad \dots (37)$$

To find the minimum of the cost function for U,

$$\frac{\partial J}{\partial U} = 0 \cdot \quad \dots (38)$$

$$\frac{\partial J}{\partial U} = -2M^T W_4 + 2M^T W_4 M U + 2W_3 U = 0 \cdot \quad \dots (39)$$

From Equation (39), the solution of the MPC is

$$\breve{U} = (M^T W_4 M + W_3) M^T W_4 S \cdot \quad \dots (40)$$

The initial parameters of the MPC were selected on the basis of theoretical practices that fit the system parameters and through manual tuning in the early simulation stages. However, PSO was later applied to tune these parameters automatically to improve the performance further and ensure optimal parameter selection, thus improving the speed and accuracy of the SBW system.

## 3.2 PSO Algorithm

The PSO algorithm can be utilised to find optimal values in various applications, most notably in PID controllers [31] [32]. However, it is rarely used in the MPC approach. PSO calculation is used in finding the optimal values of the weight matrix $W_2$, which provides accuracy and speed in reaching these values [18][19][26][33][34].

As depicted in Figure 4, the PSO process iteratively updates the position and velocity of each particle. Each particle tracks two key metrics:

$P_{best}$: the particle's best-known position based on its objective function

$g_{best}$: the best position discovered by the entire swarm

These metrics are critical in guiding particles towards the global optimum. The inertia weight, also shown in Figure 4, controls the balance between exploration and exploitation.

The inertia weight is

$$\emptyset = \emptyset_{max} - \left(\frac{\emptyset_{max} - \emptyset_{min}}{T_{max}}\right) \cdot \quad \dots (41)[35]$$

Let x and *v* be the position and velocity respectively.

The equations for updating the velocity and position are as follows:

$$v_{(i,l)}(t) = \emptyset v_{(i,l)}(t-1) + c_1 r_1 \left(P_{best} - x_{(i,l)}(t-1)\right) + c_2 r_2 \left(g_{best} - x_{(i,l)}(t-1)\right), \quad \dots (42)[36]$$

$$x_{(i,l)}(t) = x_{(i,l)}(t-1) + v_{(i,l)}(t), \quad \dots (43)[36]$$

where $c_1, c_2, i, l$ are the individual and social cognitive, number of particles and number of variations, respectively, and $r_1, r_2$ are uniformly distributed randomly. $Q_0, \dots, Q_{v-1}$ are values of the weight matrix, updated with each iteration in the partial swarm algorithm, reaching the optimal values within the predefined constraints [37][38][22].

$Q_0 = x_{(i,1)}$ , $Q_{v-1} = x_{(i,m*n)}$

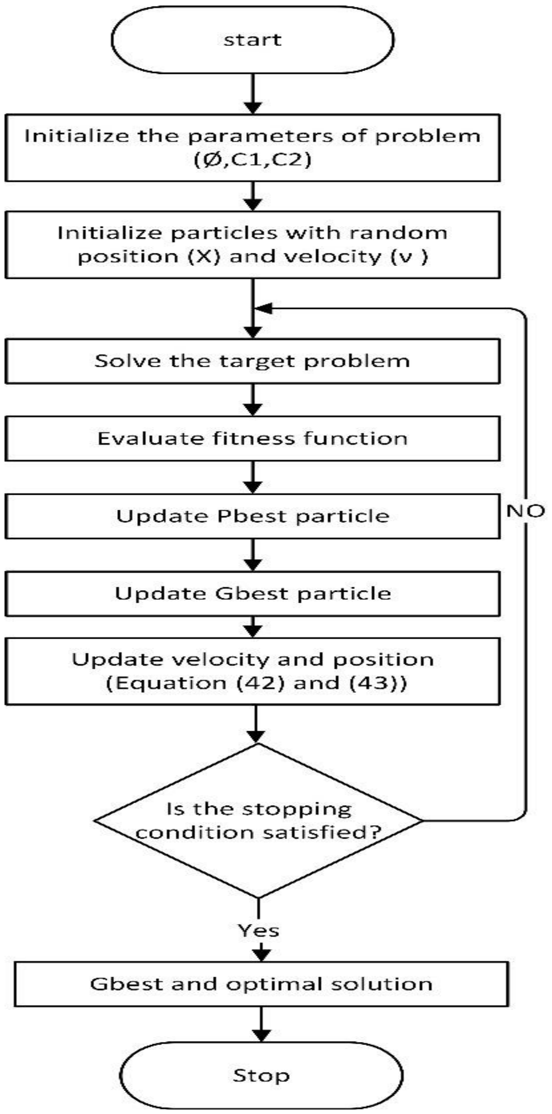


**Fig. 4. Flowchart of PSO**

**Table 1,**
**Parameters of PSO**

| Parameter | Value | Note |
|---|---|---|
| $c_1, c_2$ | 2.0 | This value represents a good balance between relying on individual experiences and global search |
| $r_1, r_2$ | Random numbers between (0,1) | To introduce stochastic behaviour |
| $\emptyset$ | 0.9 | To control the balance between exploration and exploitation |

## 4. Results and Discussion

### 4.1 Steering Wheel Simulation

The simulation was conducted on a Windows 10 PC, offering a reliable environment suitable for operating the Python 2022 programming environment.

The values mentioned in Table 3[27] were adopted as a basis for simulating the system in the absence of the PSO algorithm for the steering wheel system. The initial values of $Q_o$ and $Q_{1,v-1}$ equal to $10^{-10}$ and $10^{-9}$ respectively were chosen on the basis of the experimental tuning to balance the speed and stability in the system response as these values help in reducing overshoot whilst ensuring fast convergence. In addition, the constraints of the PSO algorithm were determined for the values [maximum value ($10^{-10}$, $10^{-2}$), minimum value ($10^{-20}$, $10^{-8}$). These constraints were chosen to ensure that the optimisation process remains within the possible and practical ranges of the system operating parameters, thus avoiding unrealistic or unstable solutions. The PSO results for the weight values $Q_o$ and $Q_{1,v-1}$ are $2.9\times10^{-4}$ and $5.1\times10^{-13}$, respectively.

#### 4.1.1 Cases of Step and Square Response

Figure 5 graphs the step response for the angle of steering motor Qm1. The use of PSO with MPC has remarkably improved the angle in terms of the settling time, which decreased from 2.096 seconds to 0.268 seconds, and overshoot decreased from 6.524% to almost 0%, as shown in Table 2. The degree of enhancement is evident in the ability to manage a square response, as illustrated in Figure 6.

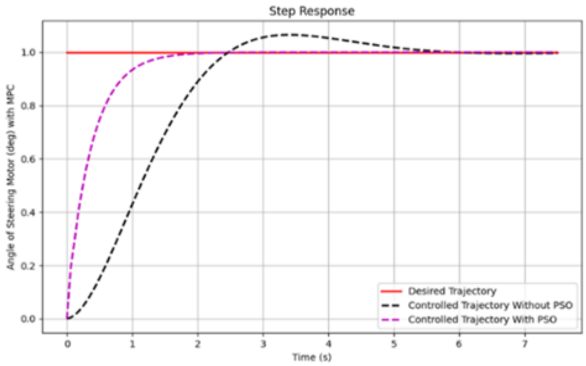


**Fig. 5. Step response for the angle of a steering motor $\Theta_{m1}$**

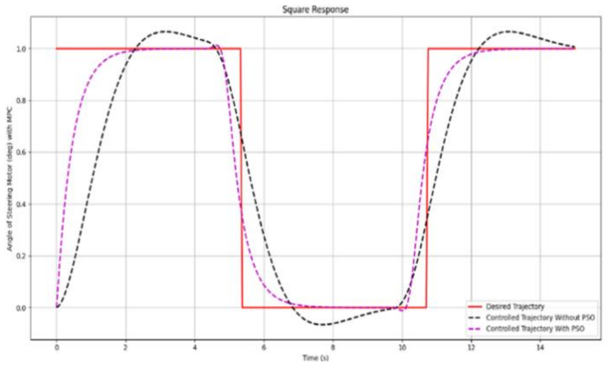


**Fig. 6. Square response for the angle of a steering motor $\Theta_{m1}$**

## 4.2 Front Wheel Simulation

In the front wheel system, the values for the weight matrix $Q_o$ and $Q_{1,v-1}$ equal to $10^{-6}$ and $10^{-3}$ respectively were employed, with constraints between a maximum of $10^{-20}$, $10^{-10}$ and a minimum of $10^{-25}$, $10^{-15}$. The obtained result of PSO for the weight values for the weight values $Q_o$ and $Q_{1,v-1}$ are $8.93\times10^{-12}$ and $9.72\times10^{-16}$, respectively.

### 4.2.1 Cases of Step and Square Response

Figure 7 shows the improvements in the angle of the front wheel motor $Q_{m2}$ when the PSO has integrated with MPC. Figure 8 shows a clear improvement in the settling time, and the rise time and the angle of the front tire $\delta_f$ can be noticed. The level of improvement appears with the same ability to deal with a square response, as shown in Figures 9 and 10.

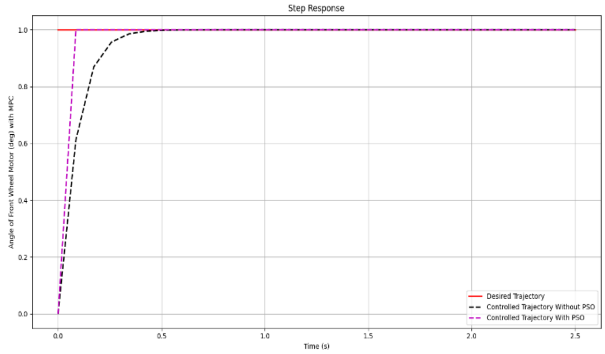


**Fig. 7. Step response for the angle of the front wheel motor $\Theta_{m2}$**

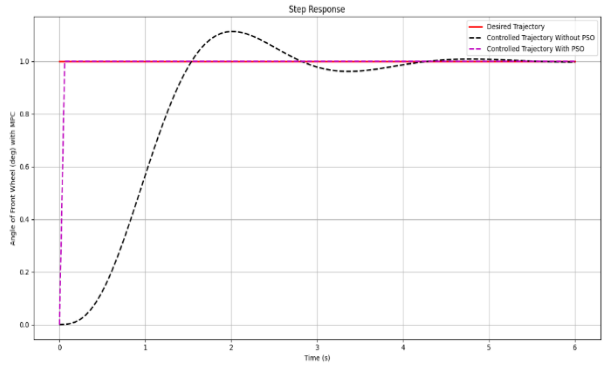


**Fig. 8. Step response for the angle of the front tire $\delta_f$**

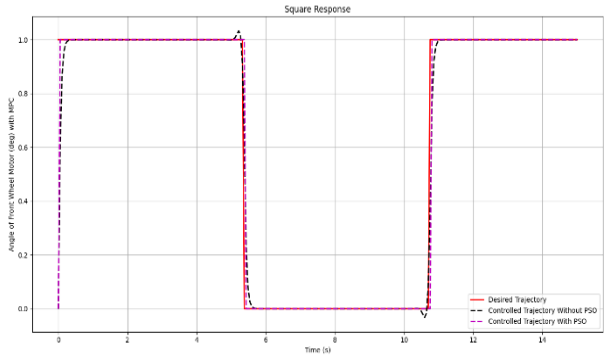


**Fig. 9. Square response for the angle of the front wheel motor $\Theta_{m2}$**

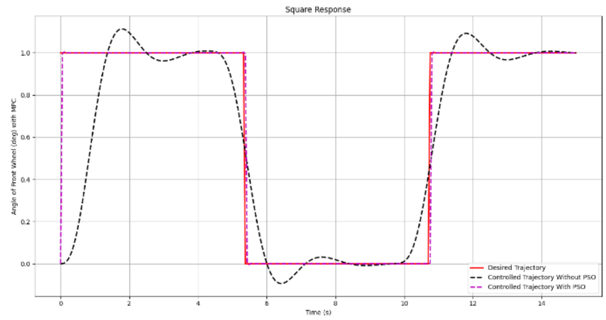


**Fig. 10. Square response for the angle of the front tire $\delta_f$.**

Comparing the results shown in Table 2 with those referenced in [19], which are considered the closest research in terms of the factors that can be compared, especially the angle of the front tire δf, revealed an improvement in settling time or overshoot. The stability time for the tire angle is 1 second, and the highest peak is 19%. The use of MPC enhanced by PSO improves this substantially, where the stability time became 0.06 seconds and the highest peak reached 0.013%, as presented in Table 2.

The MPC was trained offline using simulation data, allowing for improved tuning of parameters and testing of different scenarios before real-time implementation. The PSO algorithm was used in this offline phase to optimise the MPC parameters for robust real-time control.

## 5. Conclusion

The following points represent the conclusive findings from the present study:

1. The proposed system showed quick response through a reduction in the response time and increasing the reasonableness of real time.
2. The system focused on the MO steady state, providing high accuracy in reaching the required values without identifiable overshoot or direct safety.
3. By taking the stride of implementation indicators such as IAE and ITAE, PSO computation advances the implementation of the insight controller, making the framework more productive and responsive.
4. The frame is a suitable choice for steering systems in automobiles and other instruments that require precise control.
5. Results demonstrate good suitability for applications requiring accurate and fast responses. Furthermore, the future controller enhanced by PSO provides a good, reliable and efficient model for driving SBWs. It achieves high accuracy and fast response time in a range of real-world applications, remarkably enhancing the overall performance.

## 6. Future Development Proposal

One suitable proposal for future development of the research topic is to integrate adaptive or machine learning algorithms with PSO to adjust parameters in real time, which helps enhance control over disturbances and changing conditions and achieve the necessary robustness. Moreover, testing on real vehicles can further prove the robustness and reliability of the vehicle, offering ideas for useful implementation in automotive systems.

**Table 2,**
**Performance Indexes**

| Performance measures | MPC without PSO | | | MPC with PSO | | |
|---|---|---|---|---|---|---|
| | $\Theta_{m1}$ | $\Theta_{m2}$ | $\delta_f$ | $\Theta_{m1}$ | $\Theta_{m2}$ | $\delta_f$ |
| Settling Time (s) | 2.096 | 0.344 | 3.939 | 0.268 | 0.086 | 0.060 |
| Rise Time (s) | 1.525 | 0.188 | 0.922 | 0.179 | 0.069 | 0.048 |
| Overshoot % | 6.524 | −0.001 | 11.315 | $-1.275\times 10^{-8}$ | $1.632\times 10^{-8}$ | 0.013 |
| IAE | 1.199 | 0.093 | 1.051 | 0.090 | 0.043 | 0.030 |
| ITAE | $1.710\times 10^{-6}$ | 0.0001 | 0.066 | $6.969\times 10^{-12}$ | $3.893\times 10^{-10}$ | $1.747\times 10^{-7}$ |

**Table 3,**
**Steering-by-wire System Parameters**

| BIL | Items | Values | BIL | Items | values |
|---|---|---|---|---|---|
| $\Theta_s$ | Angular Displacement of Steering Wheel (degree) | _ | $T_{m2}$ | Front Motor Torque (N.m) | _ |
| $k_s$ | Lumped Torque Stiffness (N.m/Rad) | 3500 | $k_{b2}$ | Front Motor emf Constant (V) | 2.0 |
| $b_{sc}$ | Steering Column Damping (N.ms/Rad) | 0.136 | $b_{m2}$ | Front Motor Damping (N.m.s/Rad) | 1.0 |

| | | | | | |
|---|---|---|---|---|---|
| $J_s$ | Steering Lumped Inertia (Kg.m$^2$) | 0.0079 | $C_{m2}$ | Front Motor Shaft Compliance (N.m/s) | 0.4 |
| $\theta_{m1}$ | Angular Displacement of Front Wheel Motor (degree) | _ | $\gamma_{rack}$ | Rack Force (N.m) | _ |
| $b_{m1}$ | Motor Damping (N.m.s/Rad) | 0.05 | $br$ | Resistance Rack (N.m/Rad) | 25 |
| $J_{m1}$ | Steering Motor Inertia (Kg.m$^2$) | 2.0 | $mr$ | Mass Rack (Kg) | 2.0 |
| $T_{driver}$ | Torque of Driver (N.m) | 2.0 | $v_t$ | Tire Rod Velocity (Km/h) | _ |
| $T_{friction}$ | Torque of Friction (N.m) | 0.2 | $c_t$ | Compliance of Tire Rod (Rad/N.m) | 0.2 |
| $T_{m1}$ | Steering Motor Torque (N.m) | _ | $gr$ | Length Ratio Steering Arm (m) | 4.5 |
| $L_1$ | Steering Motor Electrical Inductance (H) | 0.0002 | $g_m$ | Column pinion Radius (m) | 0.015 |
| $R_1$ | Steering Motor Electrical Resistance (Ohm) | 4.6 | $B_t$ | Resistance of Tire Rod (N.m.s/Rad) | 0.004 |
| $i_1$ | Current of Steering Motor (A) | _ | $J_t$ | Inertia of Tire (Kg.m$^2$) | 1.36 |
| $V_{s1}$ | Power Supply Steering of Motors (V) | 12 | $\delta_f$ | Front Tire Angle (degree) | - |
| $K_{b1}$ | Steering Motor emf Constant (V) | 0.002 | $J_{m2}$ | Front Motor Inertia (Kg.m$^2$) | 0.0079 |
| $L_2$ | Front Motor Electrical Inductance (H) | 0.0002 | $i_2$ | Current of Front Motor (A) | _ |
| $R_2$ | Front Motor Electrical Resistance (Ohm) | 4.6 | $K_{b2}$ | Front Wheel Motor emf constant (V) | 2.0 |
| $K_t$ | Torque Constant (N.m/A) | 2500 | $V_{s2}$ | Power Supply Front of Motors (V) | 12 |

## References


[1] S. A. Mortazavizadeh, A. Ghaderi, M. Ebrahimi, and M. Hajian, “Recent developments in the vehicle steer-by-wire system,” *IEEE Trans. Transp. Electrif.*, vol. 6, no. 3, pp. 1226–1235, 2020.

[2] K. J. Åström and T. Hägglund, “PID controllers: theory, design, and tuning,” vol. 2. 1995.

[3] A. H. Mary, A. H. Miry, M. H. Miry, and A. H. Mary, “Design robust H ∞ -PID controller for a helicopter system using sequential quadratic programming algorithm programming algorithm,” *J. Chinese Inst. Eng.*, vol. 45, no. 8, pp. 688–696, 2022, doi: 10.1080/02533839.2022.2126401.

[4] S. Chopra, R. Mitra, and V. Kumar, “A Neurofuzzy Learning and its Application to Control system,” vol. 3, no. 1, pp. 72–78, 2005.

[5] A.H. Mary, T. Kara, and A.H. Miry, "Inverse kinematics solution for robotic manipulators based on fuzzy logic and PD control". In 2016 Al-Sadeq International Conference on Multidisciplinary in IT and Communication Science and Applications (AIC-MITCSA) (pp. 1-6). IEEE.

[6] A. H. Mary, A.H. Miry, and M.H. Miry, "System uncertainties estimation based adaptive robust backstepping control for DC DC buck converter," International Journal of Electrical & Computer Engineering (2088-8708), vol. 11,no. 1, 2021.

[7] I. Khan, “Combined lateral and longitudinal control for autonomous driving based on Model Predictive Control,” 2019.

[8] A.H. Miry, A.H. Mary, and M.H. Miry, "Mixed robust controller with optimized weighted selection for a DC servo motor". In Proceedings of the International Conference on Information and Communication Technology (pp. 178-183).2019

[9] H. Gao, T. Chen, and J. Lam, “A new delay system approach to network-based control,” *Automatica*, vol. 44, no. 1, pp. 39–52, 2008, doi: 10.1016/j.automatica.2007.04.020.

[10] A.H. Mary, A.H., Miry,and M.H. Miry, " ANFIS based reinforcement learning strategy for control a nonlinear coupled tanks system," Journal of Electrical Engineering & Technology, 17(3), pp.1921-1929.2022.

[11] S. Joe Qin and Badgwell Thomas A, “A survey of industrial model predictive control technology,” *Control Eng. Pract.*, vol. 11, pp. 733–764, 2003.

[12] M. Ali, F. Hunaini, I. Robandi, and N. Sutantra, “Optimization of active steering control on vehicle with steer by wire system using Imperialist Competitive Algorithm (ICA),” *2015 3rd Int. Conf. Inf. Commun. Technol. ICoICT 2015*, pp. 500–503, 2015, doi: 10.1109/ICoICT.2015.7231475.

[13] D. Q. Mayne, J. B. Rawlings, C. V. Rao, and P. O. M. Scokaert, “Constrained model predictive control: Stability and optimality,” *Automatica*, vol. 36, no. 6, pp. 789–814, 2000, doi: 10.1016/S0005-1098(99)00214-9.

[14] [M.-N. Nguyen *et al.*, “Model-free safety critical model predictive control for mobile robot in dynamic environments,” *IEEE Trans. Intell. Veh.*, 2024.

[15] C. Ates, D. Bicat, R. Yankov, J. Arweiler, R. Koch, and H.-J. Bauer, “Model Predictive Evolutionary Temperature Control via Neural-Network-Based

Digital Twins," *Algorithms*, vol. 16, no. 8, p. 387, 2023.

[16] N. Ye, D. Wang, and Y. Dai, "Enhancing Autonomous Vehicle Lateral Control: A Linear Complementarity Model-Predictive Control Approach," *Appl. Sci.*, vol. 13, no. 19, p. 10809, 2023.

[17] I. C. Trelea, "The particle swarm optimization algorithm: Convergence analysis and parameter selection," *Inf. Process. Lett.*, vol. 85, no. 6, pp. 317–325, 2003, doi: 10.1016/S0020-0190(02)00447-7.

[18] V. T and V. R, "Efficient Energy Load Distribution Model using Modified Particle Swarm Optimization Algorithm," *J. Artif. Intell. Capsul. Networks*, vol. 2, no. 4, pp. 226–231, 2021, doi: 10.36548/jaicn.2020.4.005.

[19] V. Kumar and V. Sharma, "Automatic voltage regulator with particle swarm optimized model predictive control strategy," *2020 1st IEEE Int. Conf. Meas. Instrumentation, Control Autom. ICMICA 2020*, pp. 0–4, 2020, doi: 10.1109/ICMICA48462.2020.9242772.

[20] S. S. Oyelere, "The Application of Model Predictive Control (MPC) to Fast Systems such as Autonomous Ground Vehicles (AGV)," *IOSR J. Comput. Eng.*, vol. 16, no. 3, pp. 27–37, 2014, doi: 10.9790/0661-16342737.

[21] M. Z. Mohd Tumari, M. S. Saealal, W. N. Abd Rashid, S. Saat, and M. A. Mohd Nasir, "The vehicle steer by wire control system by implementing PID controller," *J. Telecommun. Electron. Comput. Eng.*, vol. 9, no. 3–2, pp. 43–47, 2017.

[22] G. Huang, X. Yuan, K. Shi, Z. Liu, and X. Wu, "Adaptivity-Enhanced Path Tracking System for Autonomous Vehicles at High Speeds," *IEEE Trans. Intell. Veh.*, vol. 5, no. 4, pp. 626–634, 2020, doi: 10.1109/TIV.2020.3014776.

[23] M. Yan, W. Chen, Q. Wang, L. Zhao, X. Liang, and B. Cai, "Human–machine cooperative control of intelligent vehicles for lane keeping—considering safety of the intended functionality," *Actuators*, vol. 10, no. 9, 2021, doi: 10.3390/act10090210.

[24] V. Tavoosi, R. Kazemi, and S. M. Hosseini, "Vehicle handling improvement with steer-by-wire system using hardware in the loop method," *J. Appl. Res. Technol.*, vol. 12, no. 4, pp. 769–781, 2014, doi: 10.1016/S1665-6423(14)70093-8.

[25] R. Kazemi, I. Mousavinejad, M. Raf'at, and M. B. Kh, "Yaw Moment Control of the passenger Car via Steer by Wire system," in *ASME-International Mechanical Engneering Congress & Exposition, Denver, Colorado USA*, 2011, pp. 13–15.

[26] E. S. Mohamed and S. A. Albatlan, "Modeling and Experimental Design Approach for Integration of Conventional Power Steering and a Steer-By-Wire System Based on Active Steering Angle Control," *Am. J. Veh. Des.*, vol. 2, no. 1, pp. 32–42, 2014, doi: 10.12691/ajvd-2-1-5.

[27] S. M. H. Fahami, H. Zamzuri, S. A. Mazlan, and M. A. Zakaria, "Modeling and simulation of vehicle steer by wire system," *SHUSER 2012 - 2012 IEEE Symp. Humanit. Sci. Eng. Res.*, no. 1, pp. 765–770, 2012, doi: 10.1109/SHUSER.2012.6268992.

[28] J. Seo and K. Oh, "Model predictive control – based steering control algorithm for steering efficiency of a human driver in all-terrain cranes," vol. 11, no. 6, pp. 1–16, 2019, doi: 10.1177/1687814019859783.

[29] M. Schwenzer, M. Ay, T. Bergs, and D. Abel, "Review on model predictive control : an engineering perspective," pp. 1327–1349, 2021.

[30] J. Zhang *et al.*, "Adaptive Sliding Mode-Based Lateral Stability Control of Steer-by-Wire Vehicles with Experimental Validations," *IEEE Trans. Veh. Technol.*, vol. 69, no. 9, pp. 9589–9600, 2020, doi: 10.1109/TVT.2020.3003326.

[31] M. I. Solihin, L. F. Tack, and M. L. Kean, "Tuning of PID Controller Using Particle Swarm Optimization (PSO)," *Int. J. Adv. Sci. Eng. Inf. Technol.*, vol. 1, no. 4, p. 458, 2011, doi: 10.18517/ijaseit.1.4.93.

[32] S. Charkoutsis and M. Kara-Mohamed, "A Particle Swarm Optimization tuned nonlinear PID controller with improved performance and robustness for First Order Plus Time Delay systems," *Results Control Optim.*, vol. 12, p. 100289, 2023, doi: 10.1016/j.rico.2023.100289.

[33] *Chapter 1 Introduction to Model Predictive Control*, no. November. 2023. doi: 10.1007/978-3-030-83815-7.

[34] C. Huang, F. Naghdy, H. Du, and S. Member, "for Uncertain Steer-by-Wire System," pp. 1–12, 2017.

[35] X. Wu, J. Shen, M. Wang, and K. Y. Lee, "Intelligent predictive control of large-scale solvent-based CO2 capture plant using artificial neural network and particle swarm optimization," *Energy*, vol. 196, p. 117070, 2020, doi: 10.1016/j.energy.2020.117070.

[36] C. Huang, "Fault Tolerant Steer-by-Wire Systems : Impact on Vehicle Safety Fault Tolerant Steer-by-Wire Systems : Impact on Vehicle Safety," 2018.

[37] T. Zhang and X. Zhang, "Distributed Model Predictive Control with Particle Swarm Optimizer for Collision-Free Trajectory Tracking of MWMR Formation," *Actuators*, vol. 12, no. 3, 2023, doi: 10.3390/act12030127.

[38] M. A. Mohamed, A. M. Eltamaly, and A. I. Alolah, "PSO-based smart grid application for sizing and optimization of hybrid renewable energy systems," *PLoS One*, vol. 11, no. 8, pp. 1–22, 2016, doi: 10.1371/journal.pone.0159702.

# تحسين أداء التوجيه عن طريق الأسلاك باستخدام وحدة التحكم التنبؤية للنموذج MPC المعززة بخوارزمية تحسين سرب الجسيمات PSO

**طاهر ساجت طاهر[1] ، علي حسين مري*[2] ، فرات ابراهيم حسين[3] ، محمد غفران خضر عبوش[4] ، محمد عمر فريد[5]**

[1،2،3] *قسم هندسة الميكاترونيكس، كلية الهندسة الخوارزمي، جامعة بغداد، بغداد ، العراق*
[4] *قسم علوم البيانات والتصور، جامعة ديبريسين، المجر*
[5] *كلية ويكفيلد، ويكفيلد، انجلترا*
*البريد الالكتروني: alimary76@kecbu.uobaghdad.edu.iq

**المستخلص**

إن التحديات التي تواجه أنظمة التوجيه بالأسلاك (SBW) في المركبات ذات التوجيه ترجع إلى غياب الرابط الميكانيكي المباشر بين عجلة القيادة والعجلات على الطريق. هذا الامر يفرض ضرورة استخدام أنظمة تحكم متطورة لتحقيق أعلى درجات الدقة والاستقرار أثناء التوجيه. في مثل هذه الأنظمة، تقع المسؤولية بالكامل على وحدة التحكم المستخدمة لتغيير زاوية العجلة على الطريق بسرعة ودقة استجابة لتغييرات عجلة القيادة من قبل السائق. ومع ذلك، تعاني أنظمة التحكم التقليدية من بطء شديد في الاستجابة للتعليمات مصحوبة ببعض الأخطاء الثابتة في مرحلة الحالة المستقرة. تقدم الدراسة الحالية ابتكارًا لنموذج يدمج التحكم التنبئي بالنموذج مع تحسين سرب الجسيمات (PSO) لتحسين أداء أنظمة التوجيه بالأسلاك. يتم استخدام إجراء وحدة التحكم التنبؤية بالنموذج (MPC) عادةً للتحكم في استجابات النظام على مدى فترة زمنية والقضاء على الإجراءات غير الضرورية وغير الفعالة وفقًا للأهداف المحددة. تم استخدام خوارزمية PSO لإدارة المعلمات غير الفعالة داخل MPC. كشفت النتائج أن النهج المقترح نجح بشكل كبير وفعال في تقصير وقت الاستجابة، وتعزيز استقرار العربة، وخفض خطأ الاستقرار إلى الصفر تقريبًا. بالإضافة إلى ذلك، أدى دمج PSO مع الأداء العام للنظام إلى تحسين ضبط وقت الاستجابة، وبالتالي زيادة كفاءة النظام واستجابته. دعمت نتائج الدراسة الاقتراح المستند على أن استراتيجية التحكم يمكن أن تحسن كفاءة أنظمة SBW ذات الأهداف التشغيلية العالية.